Supramolecular Chemistry
Publication details, including instructions for authors and subscription information:
http://www.informaworld.com/smpp/title~content=t713649759

Multi-responsive cyclodextrin vesicles assembled by 'supramolecular bola-amphiphiles'

Huacheng Zhang[a]; Jian Shen[a]; Zhaona Liu[a]; Aiyou Hao[a]; Yan Bai[a]; Wei An[a]
[a] School of Chemistry and Chemical Engineering and Key Laboratory of Colloid and Interface Chemistry, Ministry of Education, Shandong University, Jinan, P.R. China

First published on: 24 February 2010

To cite this Article Zhang, Huacheng , Shen, Jian , Liu, Zhaona , Hao, Aiyou , Bai, Yan and An, Wei(2010) 'Multi-responsive cyclodextrin vesicles assembled by 'supramolecular bola-amphiphiles'', Supramolecular Chemistry, 22: 5, 297 — 310, First published on: 24 February 2010 (iFirst)
To link to this Article: DOI: 10.1080/10610270903469765
URL: http://dx.doi.org/10.1080/10610270903469765

Supramolecular Chemistry
Vol. 22, No. 5 May 2010, 297–310

Taylor & Francis
Taylor & Francis Group

Multi-responsive cyclodextrin vesicles assembled by 'supramolecular bola-amphiphiles'

Huacheng Zhang, Jian Shen, Zhaona Liu, Aiyou Hao*, Yan Bai and Wei An

School of Chemistry and Chemical Engineering and Key Laboratory of Colloid and Interface Chemistry, Ministry of Education, Shandong University, Jinan 250100, P.R. China

(*Received 19 September 2009; final version received 1 November 2009*)

Multi-responsive cyclodextrin vesicles (CDVs) self-assembled by 'supramolecular bola-amphiphiles', consisting of a guest (*N*,*N*′-bis(ferrocenylmethylene)-diaminohexane, **1**) and a host (γ-hydroxybutyric-β-cyclodextrin, γ-HB-β-CD), were prepared and investigated for the first time. The morphologies and sizes of these novel vesicles in water were observed by transmission electron microscopy (TEM), scanning electron microscopy and dynamic light scattering. The effects of the host–guest ratio, the concentration and the solvent composition are also discussed. The host–guest interactions, complex stoichiometry and structures of **1**·γ-HB-β-CD in water were investigated by cyclic voltammetry, UV and NMR spectroscopy. According to the complex stoichiometry, TEM observations and Chem3D estimation, the 'supramolecular bola-amphiphiles', made from **1**·γ-HB-β-CD and assumed for the first time, formed the membranes of the CDVs. The CDV system was responsive to an oxidising agent, which is the first report on redox-responsive systems in this field. The CDVs are also responsive to pH and the presence of metal ions, such that they disassemble upon addition of acetic acid or Cu^{2+} ions, providing possible routes to drug delivery systems.

Keywords: cyclodextrins; vesicles; non-covalently; self-assembly; supramolecular bola-amphiphiles; multi-responsive

Introduction

Vesicles, important micro-aggregates in colloid and interface chemistry, are closed membranes formed by amphiphilic compounds in solution (*1*). The conventional amphiphiles can be divided into three types according to the electrical properties of the head groups: non-ionic, anionic and cationic. The gemini- (*2*) and bola-amphiphiles (*1*, *3*, *4*) are novel amphiphiles with peculiar structures. Especially, the bola-amphiphiles, molecules with two or more hydrophilic groups connected by hydrophobic functionalities (*5*, *6*), are deemed as excellent candidates for the preparation of supramolecular structures (*7*, *8*). The vesicles assembled by bola-amphiphiles, with more stable properties and thinner membranes than vesicles formed by other amphiphiles, can serve as delivery systems for therapeutic agents and can mimic the membranes discovered in thermophilic archaebacteria (*5*).

If the vesicle-forming compounds contain cyclodextrins (CDs) or modified CDs (*9*), researchers call them cyclodextrin vesicles (CDVs) (*10*, *11*). In recent years, studies on CDVs have been the focus in supramolecular chemistry, physical chemistry and organic synthetic chemistry (*12*). According to the different composition units and formation mechanisms, the CDVs can be divided into two main types. The first type of CDVs contains CDs covalently modified with certain hydrophobic functions such as lipophilic chains and thio-alkyls (*12*). These amphiphilic CDs, non-ionic (*11*), anionic (*13*) and cationic (*14*), self-assemble by themselves into orderly bilayered membranes with the hydrophobic tails inside the bilayers and the hydrophilic heads facing the inner and outer solution medium. These CDVs have been applied to delivery of drugs (*15*) and to mimicking the recognition of biomolecules by cell membranes (*16*, *17*). Very recently, polymer-appended CDs have been used as CDV components for this type of CDVs (*18*). However, making modifications to CDs is demanding (*19*). The second type of CDVs is prepared from 'supramolecular amphiphiles', which are obtained by complexing hydrophobic guests with CDs (*19*), the versatile hosts. These CDVs easily vary their morphologies according to external stimuli (*20*). But the design principle is only to mimic the conventional amphiphiles with hydrophilic heads and hydrophobic tails. Up to now, the guest molecules used are capable of forming vesicles themselves and the available species are limited (*19*, *21*).

It should also be noted that the design strategies of CDVs have mainly been restricted to modifying or mimicking the 'heads' and 'tails' of conventional amphiphiles. The inclusion complexes between CDs and bola-/gemini-amphiphiles have been investigated by thermodynamic and spectroscopic methods (*22*). In this work, micro-aggregates based on 'supramolecular bola-amphiphiles'

*Corresponding author. Email: haoay@sdu.edu.cn

ISSN 1061-0278 print/ISSN 1029-0478 online

DOI: 10.1080/10610270903469765
http://www.informaworld.com

mechanisms are reported and their host–guest mechanisms are investigated. The guest molecule (**1**), *N*,*N*′-bis(ferrocenylmethylene)-diaminohexane, with no micro-aggregate morphology, was designed and synthesised. Recently, many functional CDs coupled with lactones have been applied to the fields (*23–25*) such as rotaxanes, drug delivery and release. To improve the aqueous solubility and inclusion ability with the guest (*26*), the native β-CD was modified here to obtain γ-hydroxybutyric-β-cyclodextrin (γ-HB-β-CD). The mixture of **1** and γ-HB-β-CD in water was observed to aggregate into vesicles by transmission electron microscopy (TEM), scanning electron microscopy (SEM) and dynamic light scattering (DLS). The host–guest interactions of **1** and γ-HB-β-CD in water were also investigated by cyclic voltammetry (CV), UV and NMR spectroscopy. The 'supramolecular bola-amphiphiles' made of **1**·γ-HB-β-CD have peculiar stimuli-responsive properties because of the ferrocene (Fc)·β-CD system (*27–33*); in particular, the CDVs prepared here were responsive to an oxidising agent. We also investigated the effect of added methanol and the response of these CDVs to addition of metal ions and to changing the pH.

Experimental

Materials

Ferrocene, 1,6-diaminohexane, sodium borohydride, γ-butyrolactone and other reagents were all commercially available from Country Medicine Reagent Co. Ltd, China. Methanol was of chromatographic purity and other organic reagents, used as received without further purification, were all of analytical purity. β-CD, recrystallised twice from distilled water and dried in vacuum for 12 h, was purchased from Guangdong Yunan Chemical Reagent Co. Ltd, China. Formylferrocene was synthesised according to the literature (*32*). All water used in the experiments was triply distilled.

Structure measurements

^{1}H NMR spectra for γ-HB-β-CD and **1** were obtained at 400 MHz on an API Bruker Avance 400 M NMR at 300 K. ^{13}C NMR spectra for γ-HB-β-CD and **1** were recorded at 75 MHz on an API Bruker Avance 300 M NMR. Positive ESI-MS scans were performed on an API 4000 MS equipment with methanol as the solvent. IR spectra were obtained on an Avatar 370 FT-IR spectrometer.

Synthesis of N,N′-bis(ferrocenylmethylene)-diaminohexane (1)

The method of synthesis of *N*,*N*′-bis(ferrocenylmethylene)-diaminohexane (**1**) was similar to that in the literature (*33*). Formylferrocene (12.84 g, 60 mmol) was reacted with 1,6-diaminohexane (HDA, 3.65 g, 31.5 mmol) in boiling absolute methanol in the presence of anhydrous K_2CO_3 (4.14 g, 30 mmol) under N_2 and protected from light for 4 h. Then, sodium borohydride (2.22 g, 60 mmol, added in several portions) was added to the reaction solution, and was reacted for another 4 h at room temperature under N_2. The crude reduction product remaining after hydrolysis with ice water (1 ml) and solvent removal (13.8 g, 90% yield) was recrystallised twice from toluene to obtain yellow powder **1** (Scheme 1). Data of **1**: mp 166–168°C; ^{1}H NMR (400 MHz, D_2O, 300 K, TMS, δ, ppm): 4.37 (d, 1H, $C_5H_2H_2$), 4.31 (d, 1H, $C_5H_2H_2$), 4.24 (s, 2.5H, C_5H_5), 4.03 (s, 1H, $C_5H_4CH_2NH$), 2.89 (t, 1H, $NHCH_2CH_2$), 1.86 (s, NH), 1.55 (t, 1H, $NHCH_2CH_2CH_2$), 1.29 (d, 1H, $NHCH_2CH_2CH_2$); ^{13}C NMR (75 MHz, D_2O, 295 K, TMS, δ, ppm): 75.89 (Fc C—C), 70.25 (Fc C—H), 69.78 (Fc C—H), 69.71 (Fc C—H), 46.99 (C—N), 46.13 (C—N), 25.16 (CH_2), 23.29 (CH_2); FT-IR (KBr plate, ν, cm^{-1}): 3446.80 (vw, br, ν_{NH}), 1614.91 (w, δ_{NH}); ESI-MS: *m*/*z* 513.4 ($M+H^+$). Anal. Calcd for $C_{28}H_{36}Fe_2N_2$ (512.29): C, 65.64; H, 7.08; N, 5.47. Found: C, 65.71; H, 7.17; N, 5.39.

Synthesis of 2-O-γ-hydroxybutyric-β-cyclodextrin

The method of synthesis of 2-*O*-γ-HB-β-CD was according to the literature (*23–25*), and the details were as follows: γ-butyrolactone (2.2 mmol, 0.18 g) was reacted with β-CD (0.88 mmol, 1.0 g) at 130°C for 24 h. The crude product was dissolved in DMF, and then the solution was added to THF (100 ml) to precipitate β-CD. The supernatant was filtered and evaporated *in vacuo* to obtain a white powder, which were then washed with acetone (3× 50 ml). The resulting powders were obtained after vacuum drying (0.17 g, 15.8% yield; Scheme 1). Data of 2-*O*-γ-HB-β-CD: ^{1}H NMR (400 MHz, D_2O, 300 K, TMS, δ, ppm): 4.93 (m, 1H, H-1), 3.82–3.43 (m, 6.51H, H-2, H-3, H-4, H-5, H-6, C═O—CH_2—, —CH_2—OH), 2.10–2.09 (m, 0.41H, —CH_2—); ^{13}C NMR (75 MHz, D_2O, 295 K, TMS, δ, ppm): 172.20 (C═O), 102.88 (C-1), 82.14 (C-4), 74.11 (C-2′), 73.09 (C-3), 72.85 (C-5), 71.40, 71.90 (C-2), 61.30 (C-6), 31.48 (CH_2), 26.69 (CH_2); ESI-MS: *m*/*z* 1239 (M^++H_2O). Anal. Calcd for $C_{46}H_{76}O_{37}$ (1221.07): C, 45.24; H, 6.27. Found: C, 45.30; H, 6.28. According to the literatures (*23–26*), ESI-MS and ^{1}H NMR, the degree of substitution is about 1.

Preparation of vesicles

Two equimolar amounts of γ-HB-β-CD powder were slowly added to a saturated aqueous solution of **1** (10^{-4} mol l^{-1}, 50 ml) and the sample solution was sonicated for 30 min at 300 K before analysis. In order to

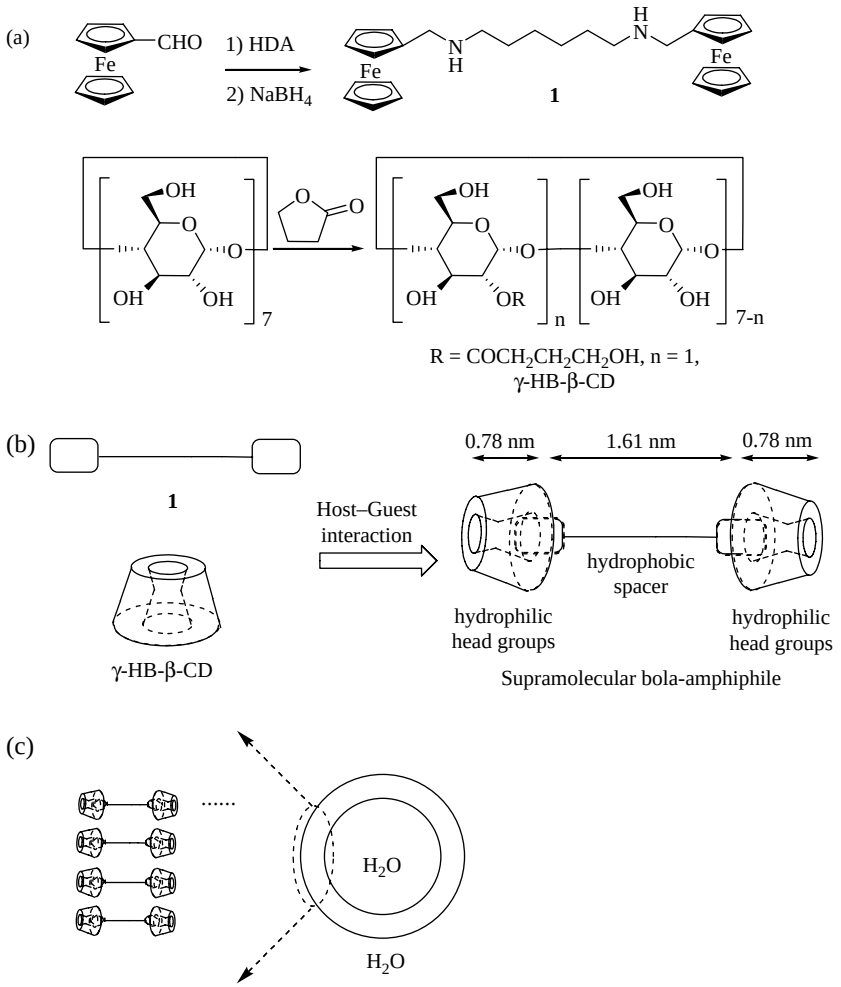

Scheme 1. (a) Synthesis of **1** and γ-HB-β-CD; models for (b) **1**, γ-HB-β-CD, supramolecular bola-amphiphile and (c) formation mechanism of vesicles.

investigate the effects of molar ratio (**1**:γ-HB-β-CD), concentration and solvent composition (water and methanol), different sample solutions were prepared by the above method. The effect of external stimuli such as an oxidant, metal ions and acid was investigated by adding NaClO, $CuCl_2$ or acetic acid to the sample solutions.

Morphological measurements

All samples for TEM were prepared by the phosphotungstic acid staining technique. A JEM-100CX II electron microscope (100 kV) was employed. SEM images were obtained on a Hitachi S-4800 scanning electron microscope after sputter-coating the TEM samples with gold.

DLS measurements were carried out with a Wyatt QELS Technology DAWN HELEOS instrument at room temperature using a 12-angle replaced detector and a 50 mW solid-state laser ($\lambda = 658.0$ nm). All solutions were filtered through a 0.45 μm filter. The experimental error was within 3 nm.

Cyclic voltammetry

CV was performed in a three-electrode cell using a model CHI650 electrochemical workstation at room temperature. A glassy carbon electrode (GCE) (3 mm in diameter) was used as the working electrode with a platinum plate as the counter electrode and a saturated calomel electrode as the reference electrode. Prior to each experiment, the GCE was first polished with α-alumina powder, then rinsed thoroughly with triply distilled water, finally sonicated in a 1:1 mixture of nitric acid and water, and triply distilled water, successively. The determination solutions were deoxygenated by bubbling with high-purity N_2 for at least 10 min before each experiment.

Ultraviolet spectra

UV spectra were recorded with a TU-1800pc UV–vis spectrophotometer at room temperature. Two equimolar stock solutions (10^{-4} mol l^{-1}), one of **1** (g) and the other of γ-HB-β-CD (h), were prepared. All sample solutions for

the investigation of inclusion phenomena were freshly prepared by diluting the stock solutions. To examine the inclusion effect, the concentration of **1** (1×10^{-5} mol l^{-1}) in the sample solutions was kept constant, but the molar ratio of γ-HB-β-CD and **1** ranged from 1:1 to 8:1.

Job's continuous variation method by UV was employed to determine the complex stoichiometry of **1**·γ-HB-β-CD at the concentration scale (10^{-5} to 10^{-4} mol l^{-1}). A set of working solutions was then obtained by mixing V_g ml of the stock **1** solution with ($V_t - V_h$) ml of the stock γ-HB-β-CD solution, where V_t is a fixed total volume and V_g is a variable value (from 0 to 10 ml, $0 \leq V_g \leq V_t$).

NMR experiments

^{1}H NMR chemical shift (δ) experiments were obtained using the API Bruker Avance 300 M NMR at 295 K referenced to the solvent peak at $\delta = 4.69$ ppm in D_2O. The 2D ^{1}H–^{1}H ROESY experiments were recorded using an INOVA-600 (600 MHz) spectrometer at ambient temperature. A mixing time of 0.200 s, a relaxation delay time of 1.000 s and an acquisition time of 0.228 s were used. All pulse sequences were set according to the company standards. Job's plot was employed to check the complex stoichiometry. Briefly, the solutions containing different molar ratios of **1** and γ-HB-β-CD with constant total molar concentration ([**1**] + [γ-HB-β-CD] = 10^{-4} mol l^{-1}) were prepared and measured.

Results and discussion

Morphologies and sizes of the CDVs

Compound **1** and γ-HB-β-CD were designed and synthesised in 90 and 15.8% yield, respectively (Scheme 1). The structures were characterised by melting point, ^{1}H NMR, ^{13}C NMR, FT-IR, ESI-MS and elemental analysis (details described in the Experimental section). Negatively stained TEM observations are reliable and versatile methods in studying micro-aggregates (*34*, *35*). The microscopic morphology of a mixture of **1** and γ-HB-β-CD (molar ratio, 1:2) in water (10^{-4} mol l^{-1}) was observed by TEM. Figure 1(a) shows the spherical structures of the micro-aggregates with vesicular shells, and the average diameter of the vesicles is about 100 nm. These observations, which are similar to those obtained by Darcy et al. (*36–39*) for hydrophobically modified CDs with alkyl chains, indicate that the thickness of the outer layer of the vesicles is about 9–12 nm. The size and size distribution of these vesicles were also detected by DLS (Figure 2), which gave an average hydrodynamic radius (R_h) of 92 nm, meaning a diameter of about 184 nm.

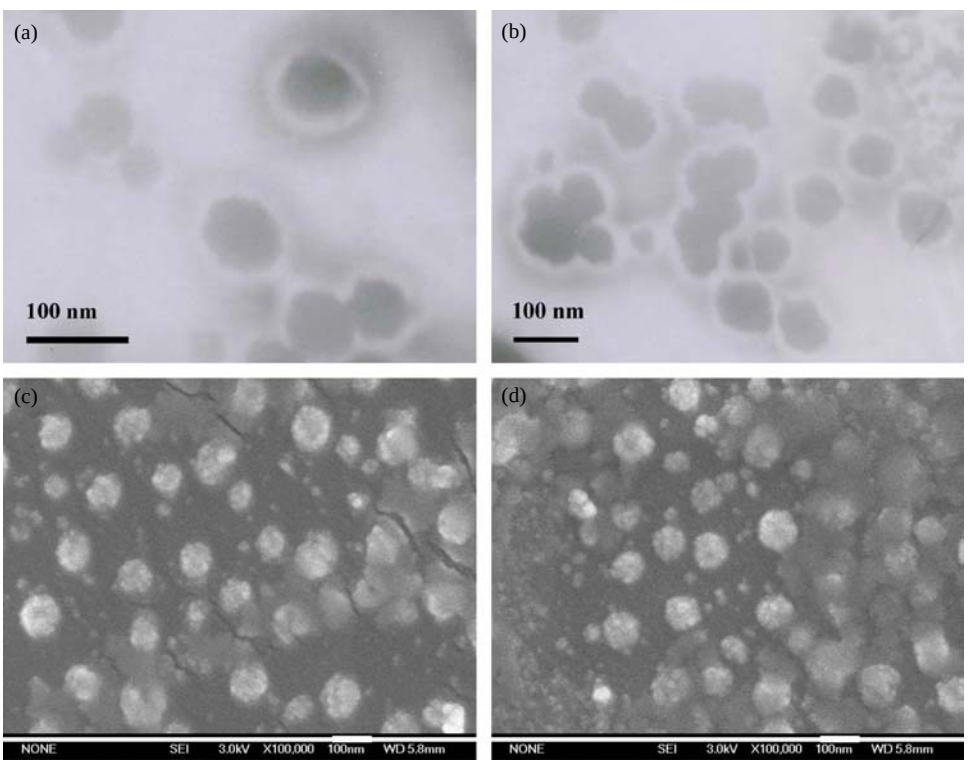

Figure 1. (a) and (b) TEM images of the mixture of **1** and γ-HB-β-CD (molar ratio, 1:2) in water (10^{-4} mol l^{-1}) with phosphotungstic acid as the negative staining agent. Scale bars, 100 nm. (c) and (d) SEM images of the micro-morphology of the above sample at room temperature.

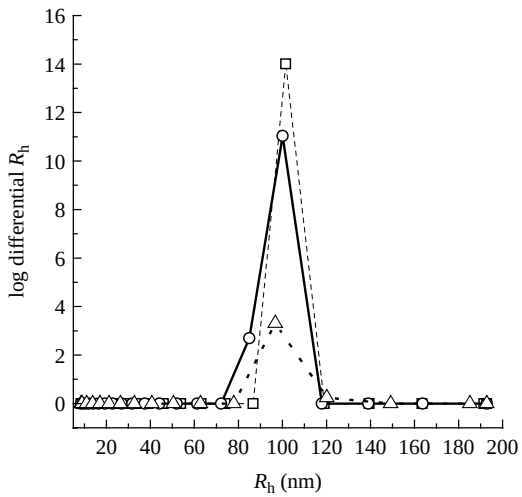

Figure 2. DLS size distributions of **1** and γ-HB-β-CD (molar ratio, 1:2) in water (□ and dashed line), the mixture of water–methanol (2:1 v/v) (○ and solid line) or methanol (Δ and dotted line).

Since TEM and DLS measure solid and swollen vesicles, respectively, the diameter of the vesicles measured by TEM is much smaller than that obtained by DLS (*20*). The sizes of these CD-containing aggregates depend critically on temperature, concentration and ultrasound intensity during sample preparation (*40*). Interestingly, the adhesion of two or several vesicles observed in Figure 1(b) by TEM resembles the process of cell fusion or cell division (*1*). Furthermore, SEM images confirm the spherical structures and the sizes of the aggregates in the 1:2 **1**:γ-HB-β-CD sample (Figure 1(c),(d)). Sputter-coating with gold can be applied to prepare organic samples for SEM (*15*, *41–43*). But during our practical operation, the sputtered gold caused damage to the surface of the micro-aggregates because of the high energy impacts (*44*). The colour contrast between the grey and white surfaces reveals that the hollow spheres collapse after drying (Figure 1).

When the molar ratio of **1** and γ-HB-β-CD varied from 1:3 to 1:6 in water, vesicles with diameters of about 100 nm can also be observed by TEM (Figure 3). The vesicular structures resemble those in the literature (*20*, *37*). The morphological differences among the vesicles (Figures 1 and 3), pointed out by Darcy (*36*), were caused by the experimental conditions and the state of the samples. The solvent composition effects on the micro-morphology were also investigated by regulating the volume ratio of water and methanol. Irregular particles are seen when using a water–methanol mixture with a volume ratio of 1:1 (Figure 4(a)) or 1:2. Vesicular aggregates are obtained in a water–methanol mixture of 2:1 (v/v) and pure methanol (Figure 4(b)–(d)). The molecular structure and polarity of methanol are analogous to water. Addition of methanol may also promote the hydrophobic parts to aggregate, leading to the formation of vesicles (*35*, *45*).

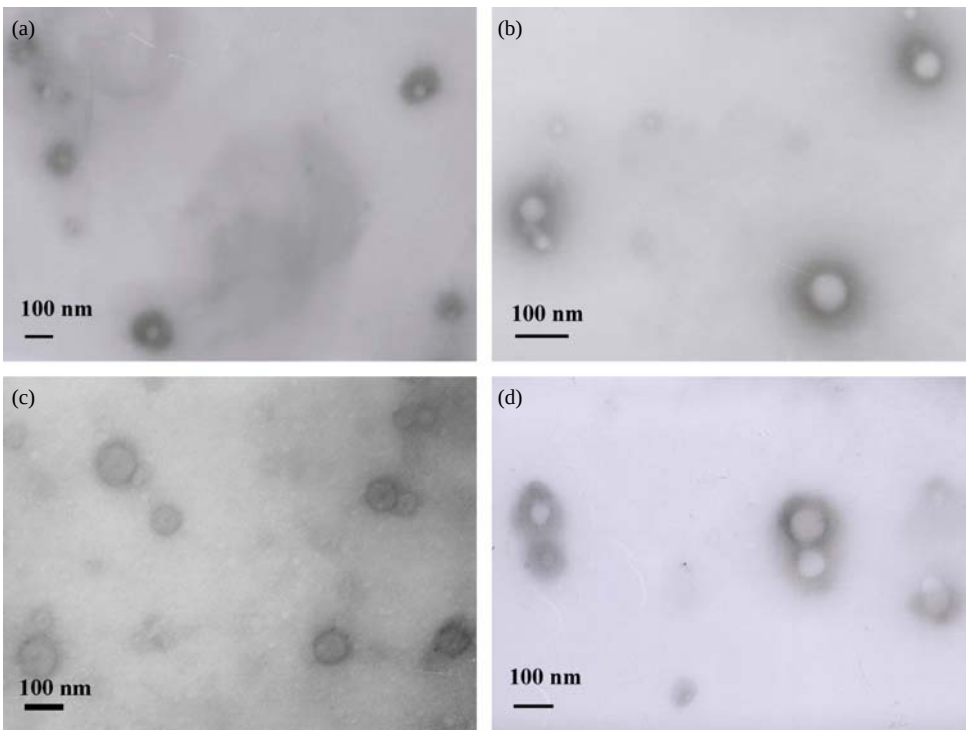

Figure 3. TEM images of the mixture of **1** and γ-HB-β-CD (molar ratio varies from 1:3 to 1:6, (a)–(d)) in water (10^{-4} mol l^{-1}) with phosphotungstic acid as the negative staining agent. Scale bars, 100 nm.

According to DLS, the R_h of the vesicles in the 2:1 (v/v) water–methanol mixture and in pure methanol are 83 and 106, respectively. The size distributions are shown in Figure 2. The lifetime of the vesicles in a pure solvent, sustainable for about 1 week at 30°C, is longer than that in a mixed solvent. In addition, no vesicles are observed by increasing or decreasing the concentration of **1** or γ-HB-β-CD in a mixed or pure solvent.

Electrochemical properties of the mixture of 1 and γ-HB-β-CD

A typical cyclic voltammogram of **1** in water at a scan rate of 25 mV s^{-1} is displayed in Figure 5(a). The reversible signal deals exclusively with the ferrocene/ferrocenium (Fc/Fc^+) redox couple. In the presence of γ-HB-β-CD (1:2), the decrease in the anodic peak current along with a shift in the anodic peak potential towards more positive values demonstrates the effective inclusion of the apolar Fc moiety of **1** in the cavity of γ-HB-β-CD (*27*, *46–50*). The decrease in the anodic peak current is caused by the fact that the wave features the oxidation of the bulky and more slowly diffusing inclusion complex. Meanwhile, the potential shift is indeed related to the fact that **1** is more difficult to oxidise in the presence of γ-HB-β-CD because its neutral form is more strongly bound than the cationic oxidised form (*28–31*).

Figure S1(a),(b) shows the cyclic voltammograms of **1** and the 1:2 mixture of **1** and γ-HB-β-CD with scan rates increasing from 25 to 150 mV s^{-1}. The plots of anodic peak currents vs. scan rates are shown in Figure 6. Linear least-square fits to the plots are all excellent, with correlation coefficients of more than 0.980. As observed, the peak current varies linearly with scan rate in **1** and the 1:2 mixture of **1** and γ-HB-β-CD (*51*, *52*). As the scan rates increase, the ΔI_p becomes larger (Figure 6). In comparison with the cyclic voltammograms of **1** and the 1:2 mixture at different scan rates (Figure 5(b)–(e)), the shifts of the anodic peak potential are similar to that obtained at 25 mV s^{-1} (Table 1). The shifts in the peak potential and the decreases in peak current at all scan rates indicate the inclusion of **1** with γ-HB-β-CD.

Formation and stoichiometry of the inclusion complex

In addition to CV, UV spectra have been effectively employed to characterise host–guest interactions (*27*). Figure 7(a) shows the typical UV spectra of **1** with the

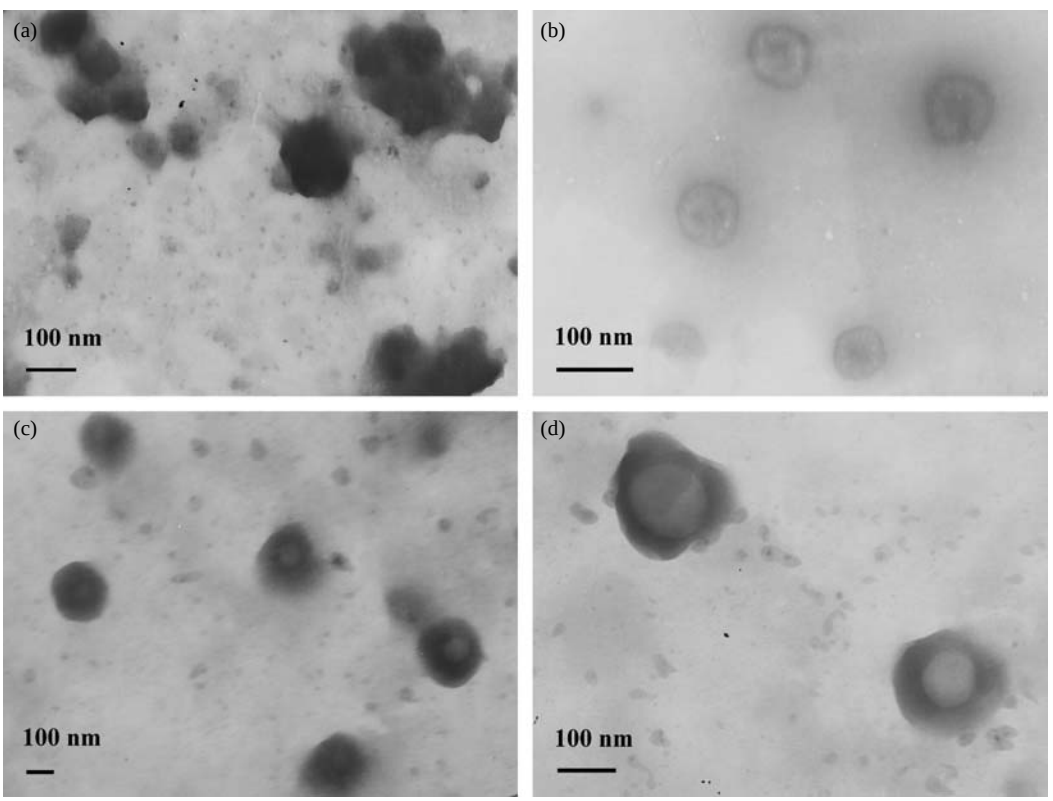

Figure 4. TEM images of the micro-morphology of **1** and γ-HB-β-CD (molar ratio, 1:2) in mixtures of water–methanol (a) 1:1, (b) 2:1 by volume and (c) and (d) different view fields of the vesicles prepared in neat methanol with phosphotungstic acid as the negative staining agent. Scale bars, 100 nm.

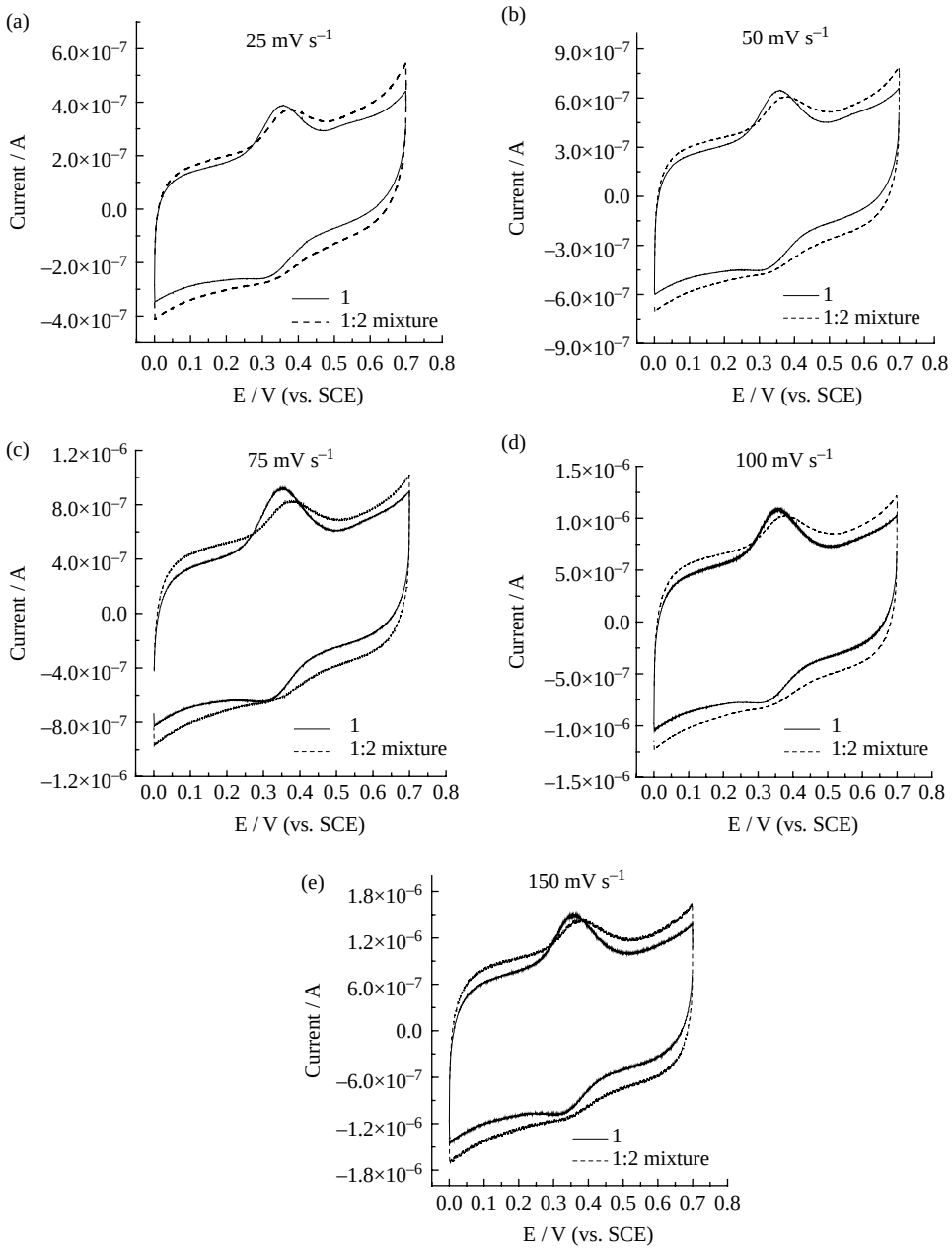

Figure 5. Cyclic voltammograms of **1** (10^{-4} mol l^{-1}) in H_2O with NaCl (0.05 mol l^{-1}) as the supporting electrolyte, recorded at a GCE (3 mm in diameter) at different scan rates of (a) 25, (b) 50, (c) 75, (d) 100 and (e) 150 mV s^{-1}, in the absence (solid line) or presence of γ-HB-β-CD (dashed line).

concentration of γ-HB-β-CD ranging from 0 to 8×10^{-5} mol l^{-1}. The intense peaks at around 190–220 nm are caused by the $\pi-\pi^*$ transfer in the cyclopentadienyl (Cp) rings and the charge transfer band between the Cp and Fe^{2+} (*53*). Small but significant changes in the absorption spectra are observed upon addition of γ-HB-β-CD to **1**, which suggests the formation of **1**·γ-HB-β-CD in solution (*54*).

The complex stoichiometry of **1**·γ-HB-β-CD in concentrations ranging from 10^{-5} to 10^{-4} mol l^{-1} was measured by means of the continuous variation method (Job's method) (*55*, *56*). The plot in Figure 7(b) shows the variations in the absorption of **1** (ΔA) with increasing molar fraction of **1**, where the total concentration of **1** and γ-HB-β-CD is kept constant at 10^{-4} mol l^{-1}. The experimental curve, describing the interactions between

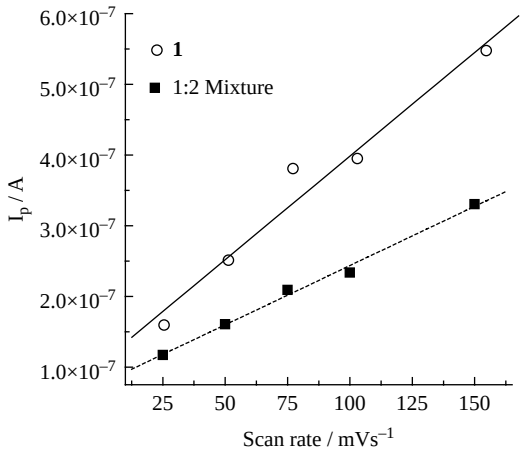

Figure 6. Plots of the anodic peak currents vs. scan rates varying from 25 to 150 mV s^{-1} in **1** (hollow symbols) and 1:2 **1**:γ-HB-β-CD sample (solid symbols).

Table 1. The anodic peak potentials of **1** and 1:2 **1**:γ-HB-β-CD sample at different scan rates.

Scan rate (mV s^{-1})	E_p (**1**)	E_p (1:2, **1**:γ-HB-β-CD)
25	0.359	0.377
50	0.359	0.376
75	0.359	0.374
100	0.358	0.377
150	0.357	0.385

1 and γ-HB-β-CD, goes through a maximum value at a molar fraction of 0.4. This indicates that the complex stoichiometry of **1**·γ-HB-β-CD is 1:2 (*57*). Job's plot shows that the complex is the most stable species in solution in accordance with similar observations reported previously (*47*, *57*). Thus, the **1**·γ-HB-β-CD complex adopted the form of G·2H when the vesicles formed.

Inclusion and spatial configurations investigated by NMR

The most direct and dependable evidence for the interaction of **1** with γ-HB-β-CD in the 1:2 **1**:γ-HB-β-CD sample was obtained using 300 MHz ^{1}H NMR (*49*, *58–62*). Figure 8 (Figure S2) shows the absorption peaks of **1** corresponding to the protons on the Fc moieties in the absence and presence of γ-HB-β-CD. In **1**, the peaks at 4.314, 4.259 and 4.184 ppm belong to Ha, Hb on the substituted Cp ring and Hc on the unsubstituted Cp ring, respectively (Figure 8). In 1:2 **1**:γ-HB-β-CD sample, the protons on the Fc moieties exhibit clear complexation-induced shifts (Δδ, Figure 8 and Table 2). In addition, the methene protons on the spacer subunit have much smaller Δδ, strongly suggesting that the Fc moieties are the active site for complexation inside the γ-HB-β-CD cavity (*49*, *50*, *55*, *57*, *58*). Meanwhile, the H3 and H1 in the 1:2 **1**:γ-HB-β-CD sample broaden, shift downfield and become well resolved in comparison with those in individual γ-HB-β-CD. The Δδ of H4 in γ-HB-β-CD is much larger than that of H6 (Table 3). These values demonstrate that the Fc moieties are included by γ-HB-β-CD through the secondary face of the CD subunit (*59–62*).

Chemical shift changes of the Cp hydrogens, Hc, were introduced to check the stoichiometry of **1**·γ-HB-β-CD by the method of continuous variation (Job's plot, Figure 9) (*57*, *63*). Its maximum at $r = [G]/([G] + [H]) = 0.4$ indicates 1:2 stoichiometry (■, dashed line) in accordance with the UV results (Figure 7(b)). This result is also confirmed by the chemical shift changes of H1. Job's plot of H1 shows a maximum at 0.3 (○, solid line). Since r is between 0.3 and 0.4, the stoichiometry of the complex is 1:2.

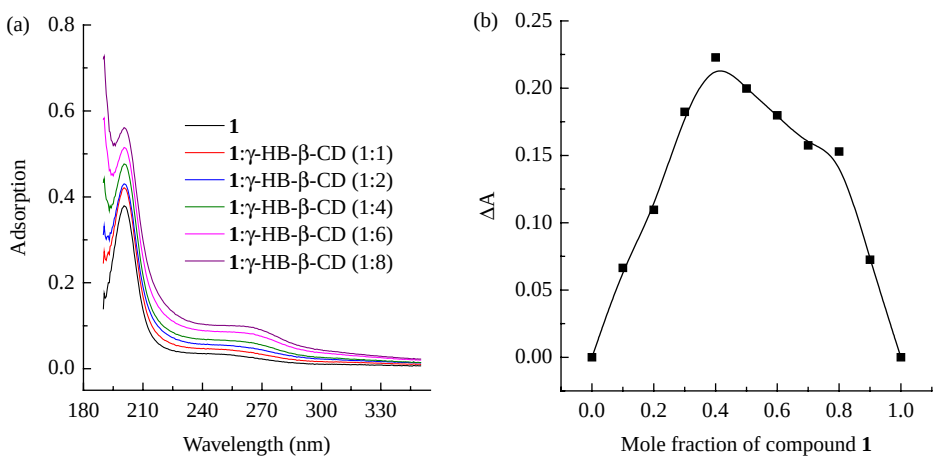

Figure 7. (a) UV spectra of **1** (1×10^{-5} mol l^{-1}) with the molar ratio (γ-HB-β-CD:**1**) ranging from 1:1 to 8:1. (b) Job's plots for binding of γ-HB-β-CD to **1** in water. [**1**] + [γ-HB-β-CD] = 10^{-4} mol l^{-1}, $T = 300$ K.

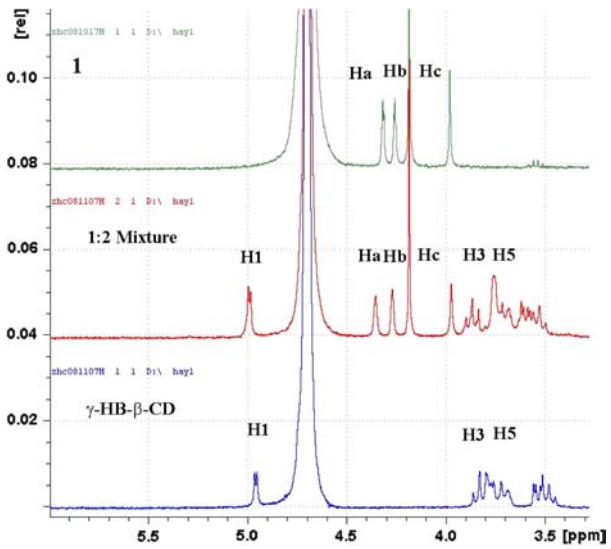

Figure 8. ^{1}H NMR spectra (300 MHz) of the 1:2 **1**:γ-HB-β-CD sample (D_2O, 10^{-4} mol l^{-1}) in comparison with the individual **1** (D_2O, 10^{-4} mol l^{-1}) and the individual γ-HB-β-CD (D_2O, 10^{-4} mol l^{-1}) at 295 K, with $\delta = 4.69$ ppm as the solvent reference.

The spatial configurations of the inclusion complex can be further confirmed by 2D NMR ROESY, which has a maximal observation limit within a spatial proximity of 5 Å (*59–62*). The selected region of the 2D NMR ROESY (600 MHz) spectrum of the 1:2 **1**:γ-HB-β-CD sample in D_2O is shown in Figure 10. The correlations between the hydrogens on the unsubstituted Cp and those inside the γ-HB-β-CD, H_3 and H_5, can be observed. This demonstrates that the Fc moieties on **1** are recognised by the cavity of γ-HB-β-CD to form the inclusion complex (*59–62*). According to the ROESY spectrum (where no correlations are observed between the hydrogens on the spacer and those on γ-HB-β-CD), $\Delta\delta$ (Tables 2 and 3) and computational calculation (*9*, *64*, *65*), the Fc moieties cannot go through the γ-HB-β-CD cavity because of the minimum internal diameter ($d_{min} = 0.58$ nm). Thus, the β-CD moieties cannot be located at the spacer subunit of **1**. Owing to its hydrophobic properties and its proximity to the Fc moieties, the methane Hd has correlations with H3. This indicates that the methene adjacent to Fc moieties is near the secondary face of the cavity (*59–62*) (Figure 10).

Formation mechanism of CDVs

No micro-aggregates were detected by TEM in the aqueous solution of individual **1** or γ-HB-β-CD. Thus, the combination of **1** and γ-HB-β-CD is crucial for vesicle formation in this system. In fact, the NMR, CV and UV data suggest the inclusion of **1** and γ-HB-β-CD. In addition, the stoichiometry of **1**·γ-HB-β-CD (1:2) indicates that the inclusion model contains two hydrophilic head groups connected by a hydrophobic spacer (Figure 10). This model resembles a bola-amphiphile, where γ-HB-β-CD molecules serve as the hydrophilic parts by host–guest interactions (Scheme 1(a)). Chem3D gives a simple estimate of about 3 nm for the inclusion size of **1**·γ-HB-β-CD (*9*, *66*). The thickness of the vesicles ($d = 9–12$ nm, Figure 1(a)) is approximately three- or fourfold the length of the supramolecular bola-amphiphile, which suggests that the objects observed are aggregates consisting of about several layers of **1**·γ-HB-β-CD (Scheme 1(b)). The mechanism of vesicle formation here is similar to the aggregates of covalent bola-amphiphiles in the literature (*7*).

For verification of the importance of the supramolecular interaction in vesicle formation, β-CD was added to the samples. When the 1:2 **1**:γ-HB-β-CD sample was mixed with 1 equivalent of β-CD in water, a small amount of vesicle-like aggregates with irregular shapes were observed by TEM (Figure 11). When the β-CD was in excess, no aggregates were observed. These phenomena could be interpreted by the inclusion equilibrium formula (Equation (1))

$$\mathbf{1}\cdot\gamma\text{-HB-}\beta\text{-CD} \overset{\beta\text{-CD}}{\rightleftharpoons} \mathbf{1}\cdot\beta\text{-CD} + \gamma\text{-HB-}\beta\text{-CD}. \qquad (1)$$

Table 2. The complexation-induced shifts ($\Delta\delta$) of the protons on **1**.

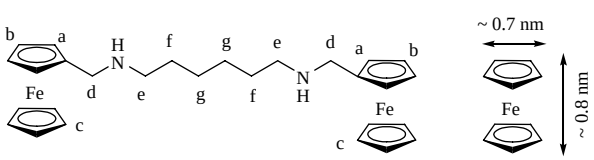

	Ha	Hb	Hc	Hd	He	Hf	Hg
$\delta_{\mathbf{1}}$	4.314	4.259	4.184	3.979	2.828	1.499	1.226
$\delta_{1:2\ \mathbf{1}:\gamma\text{-HB-}\beta\text{-CD sample}}$	4.354	4.269	4.194	3.972	2.830	1.504	1.227
$\Delta\delta^a$	0.040	0.010	0.010	−0.007	−0.002	−0.005	−0.001

[a] $\Delta\delta = \delta_{1:2\ \mathbf{1}:\gamma\text{-HB-}\beta\text{-CD sample}} - \delta_{\mathbf{1}}$.

Table 3. The complexation-induced shifts ($\Delta\delta$) of the protons on γ-HB-β-CD.

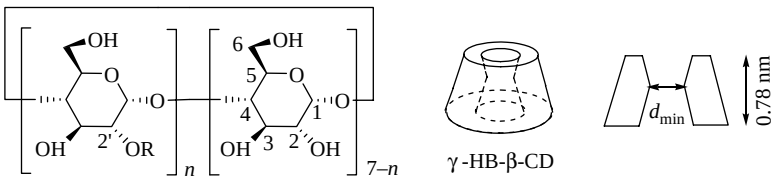

R = $COCH_2CH_2CH_2OH$,
n = 1, γ-HB-β-CD

	H1	H3	H5	H6	H4
δ_{HBCD}	4.958	3.829	3.757	3.703	3.464
$\delta_{1:2\ \mathbf{1}:\gamma\text{-HB-}\beta\text{-CD sample}}$	4.990	3.866	3.758	3.699	3.496
$\Delta\delta^a$	0.032	0.037	0.001	−0.004	0.032

[a] $\Delta\delta = \delta_{1:2\ \mathbf{1}:\gamma\text{-HB-}\beta\text{-CD sample}} - \delta_{\gamma\text{-HB-}\beta\text{-CD}}$.

The inclusion abilities of the modified β-CDs are greater than the native β-CD. However, the existence of the native β-CD in water affects **1**·γ-HB-β-CD, making the inclusion unstable (*9*, *67*). The inclusion equilibrium transfers between **1**·γ-HB-β-CD and **1**·β-CD, making the aggregates difficult to form.

Multi-responsive properties of the CDVs

The formation of host–guest complexes between Fc and β-CDs in solution has been widely investigated (*27–31*). The Fc residues are included by β-CDs, whereas the oxidised, positively charged Fc^+ moieties do not form stable complexes (*28*, *30*). Thus, the β-CDs perform as second-sphere ligands for the hydrocarbon Cp rings of the Fc (*29*), affecting the solution redox electrochemical properties, as shown in Figure 5. However, it is difficult to investigate the micro-morphologies of the 1:2 **1**:γ-HB-β-CD sample in water at the oxidation step by stopping the electrochemical process (*68*, *69*). To mimic the first step in electrochemical oxidation, a chemical oxidising agent, sodium hypochlorite solution (*70*), was mixed with the 1:2 **1**:γ-HB-β-CD sample in water. As observed by TEM, the vesicles disappear. As described in Scheme 2, the **1**·γ-HB-β-CD experiences a one-electron transfer process in which the Fc moieties are oxidised to Fc^+ moieties. Because **1**·γ-HB-β-CD is not stable enough, the aggregates in the 1:2 **1**:γ-HB-β-CD sample are disassembled.

The vesicles were observed to disappear upon addition of equimolar $CuCl_2$. The variation of peaks in the UV spectra corresponding to the Fc moieties (190–220 nm) in the presence and absence of Cu^{2+} indicates that **1** can complex this metal ion (Figure 12(a)) (*33*). Meanwhile, the UV adsorption related to the **1**·Cu^{2+} complex changes in the presence of γ-HB-β-CD (Figure 12(a)). This suggests that the γ-HB-β-CD can include the Fc moieties upon addition of Cu^{2+} (*71*, *72*). However, the addition of Cu^{2+} may alter the hydrophobic properties of the spacer, preventing hydrophobic aggregation. Thus, the presence of Cu^{2+} is harmful to the vesicles assembled by the supramolecular bola-amphiphiles (Scheme 2). In addition, the vesicles disappeared when excess acetic acid was added (*73*). The UV spectra, similar to those obtained on adding Cu^{2+}, indicate that the secondary amine may change into a quaternary ammonium, and the Fc moieties can be included by γ-HB-β-CD in the presence of H^+ (*74*) (Figure 12(b)). Meanwhile, the spacer containing the secondary amine may be disturbed upon addition of H^+, according to the literature (*75*).

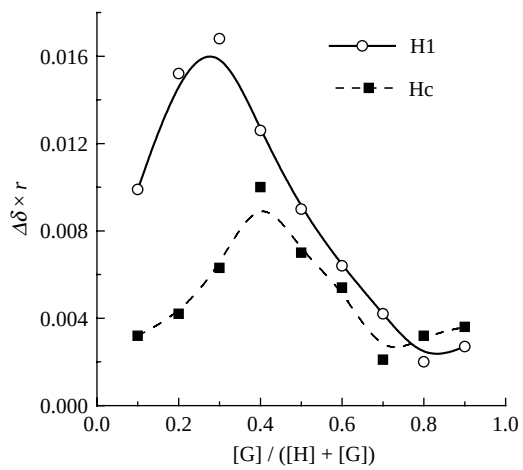

Figure 9. ^{1}H NMR Job's plot of the **1**·γ-HB-β-CD complex in D_2O. The change of the c-protons of **1** multiplied by r_1 (dashed line) and that of the H1 of γ-HB-β-CD multiplied by r_2 (solid line) are plotted on the ordinate. [**1**] + [γ-HB-β-CD] = 10^{-4} mol l^{-1}, T = 300 K, r_1 = [G]/([G] + [H]) and r_2 = [H]/([G] + [H]).

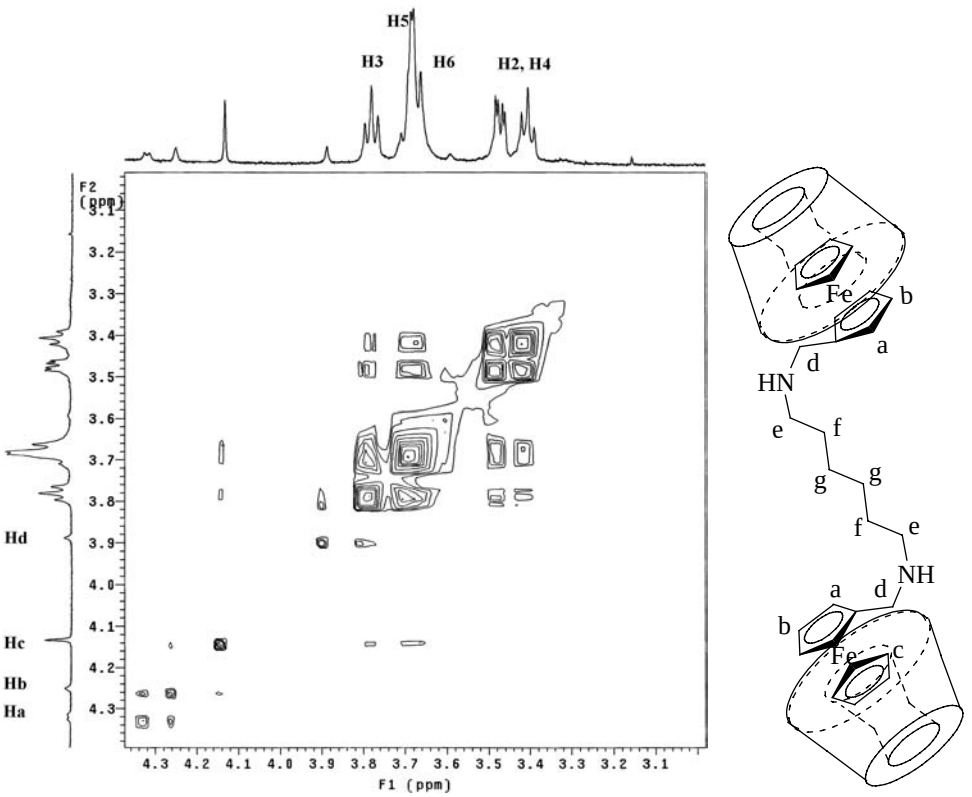

Figure 10. Selected region of the 2D NMR ROESY (600 MHz) spectrum of the 1:2 **1**:γ-HB-β-CD sample in D_2O at ambient temperature.

Therefore, the formation of a quaternary ammonium, which alters the hydrophobic properties and disturbs the spacer, is the main cause leading to the disappearance of the vesicles.

Conclusion

The significances of this paper can be summarised as follows. First, 'supramolecular bola-amphiphiles' is a novel concept. Second, 'supramolecular bola-amphiphiles' consist of the inclusion complex between the guest (**1**) and the host (γ-HB-β-CD). Third, vesicles are assembled by these 'supramolecular bola-amphiphiles', inclusion complex between the guest (**1**) and the host (γ-HB-β-CD). Neither the guest (**1**) nor the host (γ-HB-β-CD) are amphiphiles. Fourth, these vesicles have multi-responsive properties to external stimuli.

In detail, the guest (**1**) and the host (γ-HB-β-CD) were designed and synthesised. The mixture of **1** and γ-HB-β-CD in water was observed to aggregate as vesicles with a wall thickness of about 9–12 nm and diameters of about 100 nm by TEM. These observations were confirmed by SEM and DLS. The effects of the host–guest molar ratio, the concentration and the solvent composition were also investigated by TEM and DLS. In addition, CV, UV and ^{1}H NMR results indicate that **1** and γ-HB-β-CD can form a **1**·γ-HB-β-CD complex in water. The complex structures such as recognition sites and spatial configurations were investigated by ^{1}H and 2D

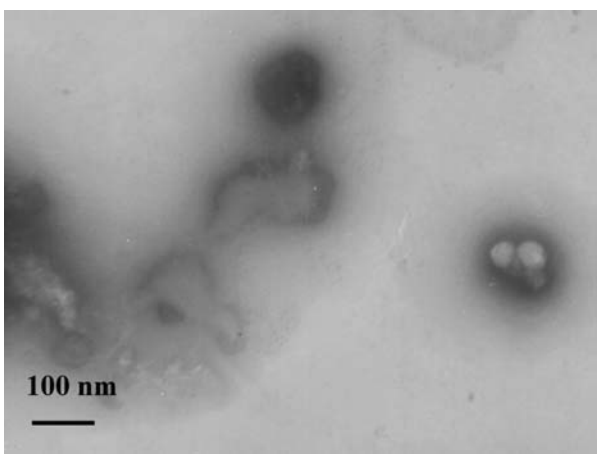

Figure 11. TEM images of the mixture of **1**, γ-HB-β-CD and β-CD (molar ratio, 1:2:2) in water (10^{-4} mol l^{-1}) with phosphotungstic acid as the negative staining agent. Scale bar, 100 nm.

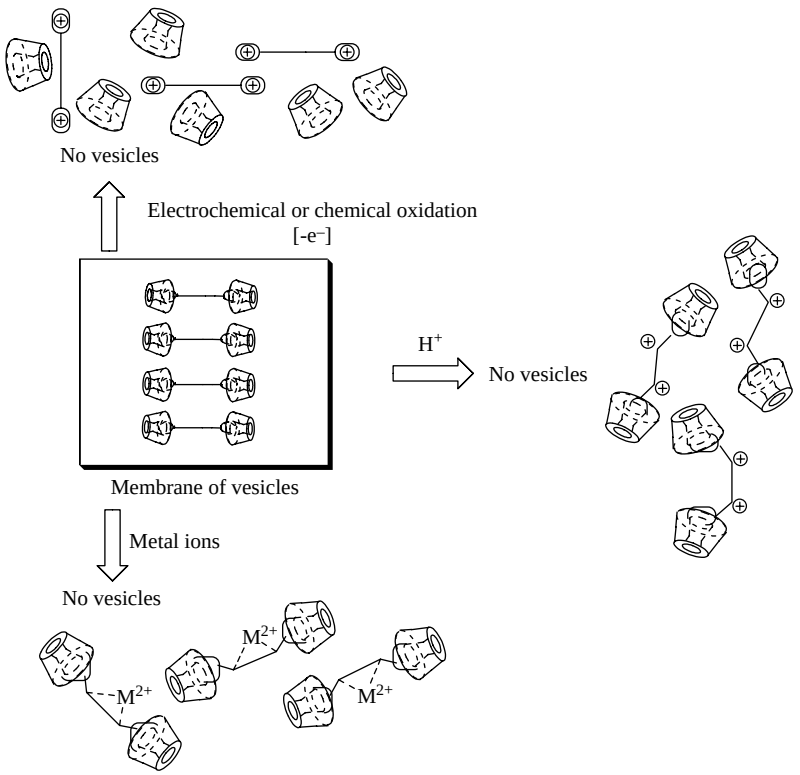

Scheme 2. Illustration of the disappearance of the vesicles upon electrochemical/chemical oxidation and addition of metal ions.

ROESY NMR. According to the complex stoichiometry (1:2) obtained by Job's method from the UV and ^{1}H NMR data, the 'supramolecular bola-amphiphiles' made by **1**·γ-HB-β-CD were deemed to be the composition units of the CDVs. Moreover, given the three- or fourfold length of **1**·γ-HB-β-CD estimated by Chem3D, in accordance with the vesicle thickness, a vesicle model consisting of several layers is suggested.

The vesicular systems responded to an oxidising agent, which is the first report on redox-responsive systems in CDVs. These are the first CDVs to be reported which are stable in the presence of methanol. In addition,

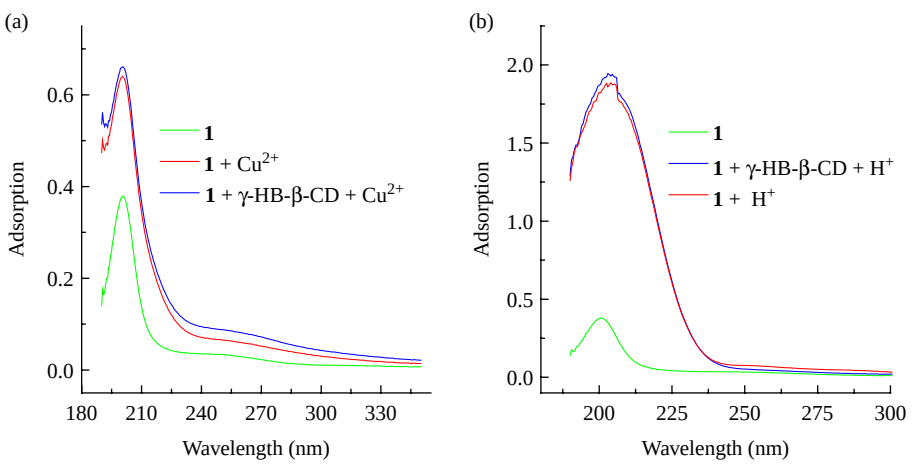

Figure 12. (a) UV spectra of **1** (green line), the mixture of **1** and $CuCl_2$ (red line), the mixture of **1**, γ-HB-β-CD and $CuCl_2$ (blue line). [**1**] = [Cu^{2+}] = [γ-HB-β-CD] = 10^{-5} mol l^{-1}. (b) UV spectra of **1** (green line), the mixture of **1** and acetic acid (red line), the mixture of **1**, γ-HB-β-CD and acetic acid (blue line). [**1**] = [γ-HB-β-CD] = 10^{-5} mol l^{-1}. T = 300 K.

the CDVs could disassemble after addition of Cu^{2+} ions or acetic acid. The disassembly mechanisms were investigated by UV spectroscopy. All these multi-responsive properties could be significant in developing novel drug delivery systems and mimicking natural biological membranes.

Acknowledgements

The authors are grateful for the financial support of the NSFC (Grant No. 20625307, J. Hao) and National Basic Research Program of China (973 Program, 2009CB930103). We are grateful to Prof. Dr Jingcheng Hao and Prof. Dr Ganzuo Li from Key Laboratory of Colloid and Interface Chemistry for assistance with their helpful discussions and financial supports.

Supplementary Material

Details of the cyclic voltammograms of **1** and 1:2 **1**:γHB-β-CD sample at different scan rates in $mV\,s^{-1}$ and ^1H NMR spectra (300 MHz) of the 1:2 **1**:γ-HB-β-CD sample in comparison with **1** and γ-HB-β-CD alone.

References

(1) Fuhrhop, J.H.; Mathieu, J. *Angew. Chem. Int. Ed. Engl.* **1984**, *23*, 100–113.
(2) Menger, F.M.; Littau, C.A. *J. Am. Chem. Soc.* **1991**, *113*, 1451–1452.
(3) Sun, J.K.; Yu, H.; Russo, P.S.; Pople, J.; Henry, A.; Lyles, B.; McCarley, R.S.; Baker, G.R.; Newkome, G.R. *A.C.S. Symp. Ser.* **2006**, *918*, 370–383.
(4) Shimizu, T.; Masuda, M.; Minamikawa, H. *Chem. Rev.* **2005**, *105*, 1401–1443.
(5) Escamilla, G.H.; Newkome, G.R. *Angew. Chem. Int. Ed. Engl.* **1994**, *33*, 1937–1940.
(6) Fuhrhop, J.H.; Fritsch, D. *Acc. Chem. Res.* **1986**, *19*, 130–137.
(7) Ambrosi, M.; Fratini, E.; Alfredsson, V.; Ninham, B.W.; Giorgi, R.; Nostro, P.L.; Baglioni, P. *J. Am. Chem. Soc.* **2006**, *128*, 7209–7214.
(8) Mstsui, H.; Douberly, G.E. *Langmuir* **2001**, *17*, 7918–7922.
(9) Szejtli, J. *Chem. Rev.* **1998**, *98*, 1743–1754.
(10) Bugler, J.; Sommerdijk, N.A.J.M.; Visser, A.J.W.G.; Hoek, A.; Nolte, R.J.M.; Engbersen, J.F.J.; Reinhoudt, D.N. *J. Am. Chem. Soc.* **1999**, *121*, 28–33.
(11) Ravoo, B.J.; Darcy, R. *Angew. Chem. Int. Ed.* **2000**, *39*, 4324–4326.
(12) Sallas, F.; Darcy, R. *Eur. J. Org. Chem.* **2008**, *6*, 957–969.
(13) Sukegawa, T.; Furuike, T.; Niikura, K.; Yamagishi, A.; Monde, K.; Nishimura, S.I. *Chem. Commun.* **2002**, 430–431.
(14) Donohue, R.; Mazzaglia, A.; Ravoo, B.J.; Darcy, R. *Chem. Commun.* **2002**, 2864–2865.
(15) Mazzaglia, A.; Angelini, N.; Lombardo, D.; Micali, N.; Patane, S.; Villari, V.; Scolaro, L.M. *J. Phys. Chem. B* **2005**, *109*, 7258–7265.
(16) Ravoo, B.J.; Jacquier, J.C.; Wenz, G. *Angew. Chem. Int. Ed.* **2003**, *42*, 2066–2070.
(17) Lim, C.W.; Ravoo, B.J.; Reinhoudt, D.N. *Chem. Commun.* **2005**, 5627–5629.
(18) Felici, M.; Perez, M.M.; Hatzakis, N.S.; Nolte, R.J.M.; Feiters, M.C. *Chem. Eur. J.* **2008**, *14*, 9914–9920.
(19) Jing, B.; Chen, X.; Wang, X.; Yang, C.; Xie, Y.; Qiu, H. *Chem. Eur. J.* **2007**, *13*, 9137–9142.
(20) Zou, J.; Tao, F.; Jiang, M. *Langmuir* **2007**, *23*, 12791–12794.
(21) Park, C.; Lim, J.; Yun, M.; Kim, C. *Angew. Chem. Int. Ed.* **2008**, *47*, 2959–2963.
(22) Gonzalez-Gaitano, G.; Guerrero-Martinez, A.; Ortega, F.; Tardajos, G. *Langmuir* **2001**, *17*, 1392–1398.
(23) Harada, A.; Osaki, M.; Takashima, Y.; Yamaguchi, H. *Acc. Chem. Res.* **2008**, *41*, 1143–1152.
(24) Osaki, M.; Takashima, Y.; Yamaguchi, H.; Harada, A. *J. Am. Chem. Soc.* **2007**, *129*, 14452–14457.
(25) Osaki, M.; Takashima, Y.; Yamaguchi, H.; Harada, A. *Macromolecules* **2007**, *40*, 3154–3158.
(26) Khan, A.R.; Forgo, P.; Stine, K.J.; D'Souza, V.T. *Chem. Rev.* **1998**, *98*, 1977–1996.
(27) Matsue, T.; Evans, D.H.; Osa, T.; Kobayashi, N. *J. Am. Chem. Soc.* **1985**, *107*, 3411–3417.
(28) Kaifer, A.E. *Acc. Chem. Res.* **1999**, *32*, 62–71.
(29) Hapiot, F.; Tilloy, S.; Monflier, E. *Chem. Rev.* **2006**, *106*, 767–781.
(30) Harada, A. *Acc. Chem. Res.* **2001**, *34*, 456–464.
(31) Kaifer, A.E. *Eur. J. Inorg. Chem.* **2007**, *32*, 5015–5027.
(32) Sato, M.; Kono, H.; Shiga, M.; Motoyama, I. *Bull. Chem. Soc. Jpn.* **1986**, *41*, 252.
(33) Neuse, E.W.; Meirim, M.G.; Blom, N.F. *Organometallics* **1988**, *7*, 2562–2565.
(34) He, Y.; Fu, P.; Shen, X.; Gao, H. *Micron* **2008**, *39*, 495–516.
(35) Wang, L.; Liu, H.; Hao, J. *Chem. Commun.* **2009**, 1353–1355.
(36) McNicholas, S.; Rencurosi, A.; Lay, L.; Mazzaglia, A.; Sturiale, L.; Perez, M.; Darcy, R. *Biomacromolecules* **2007**, *8*, 1851–1857.
(37) Mazzaglia, A.; Forde, D.; Garozzo, D.; Malvagna, P.; Ravoo, B.J.; Darcy, R. *Org. Biomol. Chem.* **2004**, *2*, 957–960.
(38) Falvey, P.; Lim, C.W.; Darcy, R.; Revermann, T.; Karst, U.; Giesbers, M.; Marcelis, A.T.M.; Lazar, A.; Coleman, A.W.; Reinhoudt, D.N.; Ravoo, B.J. *Chem. Eur. J.* **2005**, *11*, 1171–1180.
(39) Nolan, D.; Darcy, R.; Ravoo, B.J. *Langmuir* **2003**, *19*, 4469–4472.
(40) Mazzaglia, A.; Ravoo, B.J.; Darcy, R.; Gambadauro, P.; Mallamace, F. *Langmuir* **2002**, *18*, 1945.
(41) Qian, J.; Wu, F. *Macromolecules* **2008**, *41*, 8921–8926.
(42) Abdelwahed, W.; Degobert, G.; Dubes, A.; Parrot-Lopez, H.; Fessi, H. *Int. J. Pharm.* **2008**, *351*, 289–295.
(43) Yang, J.; Keller, M.W.; Moore, J.S.; White, S.R.; Sottos, N.R. *Macromolecules* **2008**, *41*, 9650–9655.
(44) Yuan, P.; Yang, S.; Wang, H.; Yu, M.; Zhou, X.; Lu, G.; Zou, J.; Yu, C. *Langmuir* **2008**, *24*, 5038–5043.
(45) Huang, J.B.; Zhu, B.Y.; Zhao, G.X.; Zhang, Z.Y. *Langmuir* **1997**, *13*, 5759–5761.
(46) Buriez, O.; Heldt, J.M.; Labbe, E.; Vessieres, A.; Jaouen, G.; Amatore, C. *Chem. Eur. J.* **2008**, *14*, 8195–8203.
(47) Mendoza, S.; Castano, E.; Meas, Y.; Godinez, L.A.; Kaifer, A.E. *Electroanalysis* **2004**, *16*, 1469–1477.
(48) Osella, D.; Carretta, A.; Nervi, C.; Ravera, M.; Gobetto, R. *Organometallics* **2000**, *19*, 2791–2797.
(49) Isnin, R.; Salam, C.; Kaifer, A.E. *J. Org. Chem.* **1991**, *56*, 35–41.
(50) Ashton, P.R.; Balzani, V.; Clemente-Leon, M.; Colonna, B.; Credi, A.; Jayaraman, N.; Raymo, F.M.; Stoddart, J.F.; Venturi, M. *Chem. Eur. J.* **2002**, *8*, 673–684.

(51) Vergheese, T.M.; Berchmans, S. *Electrochim. Acta* **2006**, *52*, 567–574.
(52) Rojas, M.T.; Koniger, R.; Stoddart, J.F.; Kaifer, A.E. *J. Am. Chem. Soc.* **1995**, *117*, 336–343.
(53) Kobayashi, N.; Opallo, M. *J. Chem. Soc. Chem. Commun.* **1990**, 477–479.
(54) Cramer, F.; Saenger, W.; Spatz, H.C. *J. Am. Chem. Soc.* **1967**, *89*, 14–21.
(55) Song, L.X.; Wang, H.M.; Guo, X.Q.; Bai, L. *J. Org. Chem.* **2008**, *73*, 8305–8316.
(56) Shen, J.; Hao, A.; Du, G.; Zhang, H.; Sun, H. *Carbohyd. Res.* **2008**, *343*, 2517–2522.
(57) Denadai, A.M.L.; Teixeira, K.I.; Santoro, M.M.; Pimenta, A.M.C.; Cortes, M.E.; Sinisterra, R.D. *Carbohyd. Res.* **2007**, *342*, 2286–2296.
(58) Schneider, H.J.; Hacket, F.; Rudiger, V.; Ikeda, H. *Chem. Rev.* **1998**, *98*, 1755–1785.
(59) Liu, J.; Alvarez, J.; Ong, W.; Roman, E.; Kaifer, A.E. *J. Am. Chem. Soc.* **2001**, *123*, 11148–11154.
(60) Liu, W.; Xie, T.; Liang, Y.; Liu, W.; Ma, Y. *J. Organomet. Chem.* **2001**, *627*, 93–98.
(61) Skinner, P.J.; Blair, S.; Kataky, R.; Parker, D. *New J. Chem.* **2000**, *24*, 265–268.
(62) Han, Y.; Cheng, K.; Simon, K.A.; Lan, Y.; Sejwal, P.; Luk, Y.Y. *J. Am. Chem. Soc.* **2006**, *128*, 13913–13920.
(63) Walla, P.; Arion, V.B.; Brinker, U.H. *J. Org. Chem.* **2006**, *71*, 3274–3277.
(64) Wenz, G.; Han, B.; Muller, A. *Chem. Rev.* **2006**, *106*, 782–817.
(65) Sabapathy, R.C.; Bhattacharyya, S.; Cleland, W.E.; Hussey, C.L. *Langmuir* **1998**, *14*, 3797–3807.
(66) Zhong, D.Y.; Franke, J.; Blomker, T.; Erker, G.; Chi, L.F.; Fuchs, H. *Nano. Lett.* **2009**, *9*, 132–136.
(67) Connors, K.A. *Chem. Rev.* **1997**, *97*, 1325–1358.
(68) Nijhuis, C.A.; Huskens, J.; Reinhoudt, D.N. *J. Am. Chem. Soc.* **2004**, *126*, 12266–12267.
(69) Nijhuis, C.A.; Ravoo, B.J.; Huskens, J.; Reinhoudt, D.N. *Coordin. Chem. Rev.* **2007**, *251*, 1761–1780.
(70) Tomatsu, I.; Hashidazume, A.; Harada, A. *Macomol. Rapid Commun.* **2006**, *27*, 238–241.
(71) Petrovski, Z.; Braga, S.S.; Santos, A.M.; Rodrigues, S.S.; Goncalves, I.S.; Pillinger, M.; Kuhn, F.E.; Romao, C.C. *Inorg. Chim. Acta* **2005**, *358*, 981–988.
(72) Petrovski, Z.; Braga, S.S.; Santos, A.M.; Rodrigues, S.S.; Pereira, C.C.L.; Goncalves, I.S.; Pillinger, M.; Freire, C.; Romao, C.C. *New J. Chem.* **2005**, *29*, 347–354.
(73) Micali, N.; Villari, V. *Phys. Rev. E* **2006**, *73*, 051904, 1–8.
(74) Isnin, R.; Kaifer, A.E. *J. Am. Chem. Soc.* **1991**, *113*, 8188–8190.
(75) Ludden, M.J.W.; Reinhoudt, D.N.; Huskens, J. *Chem. Soc. Rev.* **2006**, *35*, 1122–1134.